D2.1 – OLET technology and parameters

Project Information

Grant Agreement Number	780839
Project Full Title	Multiplex phOtonic sensor for pLasmonic-based Online detection of contaminants in milK
Project Acronym	MOLOKO
Funding scheme	IA
Start date of the project	January 1st, 2018
Duration	42 months
Project Coordinator	Stefano TOFFANIN (CNR)
Project Website	http://www.moloko-project.eu

Deliverable Information

Deliverable n°	2.1
Deliverable title	OLET technology and parameters
WP no.	2
WP Leader	CNR
Contributing Partners	CNR, PLAS, FhG (FEP)
Nature	R
Authors	Mario PROSA (CNR)
Contributors	Michael TOERKER (Fraunhofer-FEP)
Reviewers	Stefano TOFFANIN (CNR)
Contractual Deadline	September 30th 2018
Delivery date to EC	October 4th 2018

Dissemination Level

PU	Public	✓
PP	Restricted to other programme participants (incl. Commission Services)	
RE	Restricted to a group specified by the consortium (incl. Commission Services)	
CO	Confidential, only for the members of the consortium (incl.CommissionServices)	

Document Log

Version	Date	Author	Description of Change
V1.0	25/09/2018	Mario Prosa (CNR)	First draft of the document
V1.1	01/10/2018	Michael Toerker (FhG FEP), Paola Pellacani (PLAS)	General revision
V2.0	03/20/2018	Stefano Toffanin	Final revision

Table of Contents

1 Executive Summary

Work package (WP) 2 aims at the production of the organic photonic module to be integrated in the MOLOKO sensor. In particular, WP2 focuses on the development of organic light-emitting transistors (OLETs) and organic photodiodes (OPDs) representing, respectively, the light-source and the light-detector of the organic photonic module. The two elements are monolithically integrated and, in conjunction with the nanoplasmonic grating (WP3), compose the optoplasmonic chip, that is, the core of the MOLOKO detection scheme to reveal biochemical inputs.
Following the specifications presented in the Deliverable 1.1 (D1.1) "*Specification statement for photonic, plasmonic and microfluidic modules and for production of the automatic-controlled MOLOKO sensor*" of WP1 and, according to the guidelines provided by the Task 1.2 (T1.2) "*Design of optoplasmonic module*" of WP1, WP2 aims at the development of the OLET technology (T2.1), the development of the OPD technology (T2.2) and their integration towards a final batch production (T2.3, T2.4, T2.5 and T2.6).

In accordance to the contents of T2.1 "*OLET Development*", D2.1 focuses on the design, fabrication and optimization of the OLET technology in terms of device architectures, figures-of-merit (FOMs) and spectral characteristics.

In this document, Chapter 2 provides a general overview of the OLET composition, geometry and characteristics.

Chapter 3 describes the development of the OLET technology according to the MOLOKO requirements. In particular, the selected spectral characteristics of OLETs are presented and discussed in paragraph 3.1 while the progresses in terms of architecture and operating conditions of the devices are reported in paragraphs 3.2 and 3.3, respectively.

2 Background of the OLET technology

OLETs constitute the light-emitting source of the MOLOKO optoplasmonic chip. Similar to organic light-emitting diodes (OLEDs), OLETs are multi-layered devices where light is generated from an organic emissive material in the three-electrode geometry typical of transistors (differently from organic light-emitting diodes - OLEDs). Indeed, OLETs present further fascinating characteristics due to the use of a third electrode, which confers to OLETs the electrical switch capability typical of organic field-effect transistors (OFETs). Thus, OLETs can be defined as OFETs able to emit light.

In details, OLETs are endowed with an organic emissive layer sandwiched between an organic charge-transporting semiconductor, which drives majority charges, and an injecting electrode for minority charges named as "*drain*" (D). The OLET architecture is completed by an insulating layer placed between the organic semiconducting layer and a *gate* electrode (G), while a *source* electrode (S) is deposited over the organic semiconductor planar and at a certain distance (OLET channel) with respect to the drain electrode (Figure 1).

The application of a gate-source bias (V_{GS}) over a certain threshold voltage (V_{TH}) populates the organic semiconductor (at the interface with the dielectric layer) with majority charges. A horizontal charges flow is activated by the application of a drain-source bias (V_{DS}). Hence, majority charges are injected into the organic emissive layer where radiatively recombine with opposite minority charges injected from the drain electrode with the generation of light. Due to the use of a reflective drain electrode, light is directed to the bottom side of the device, passing through a transparent glass substrate. It is worth mentioning that a suitable selection of materials is necessary to fulfil the energetic requirements and to ensure all the described processes.

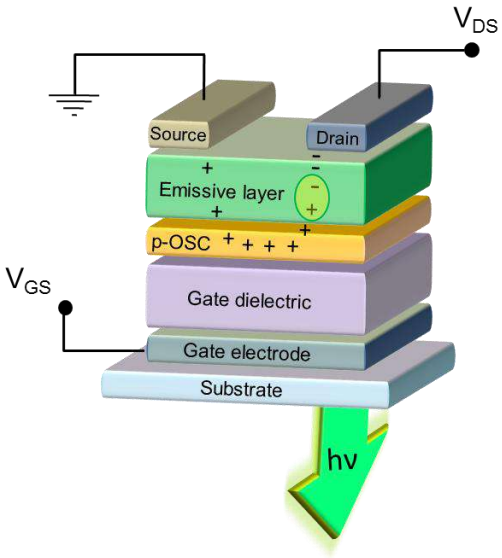

Figure 1. Schematic representation of an OLET device structure where a p-type organic material is used as semiconductor (p-OSC).

Except the gate dielectric, all the materials are deposited by thermal evaporation in high vacuum by using shadow masks. The gate dielectric, typically poly(methyl methacrylate) (PMMA), is deposited by solution and then post-treated with a thermal curing treatment. All the other organic layers do not require any post-treatment. As reported in the D1.1, the described architecture (Figure 1), named as "bilayer OLET", represents an optimal compromise to keep low the degree of manufacture complexity while maintaining great optoelectronic characteristics of OLETs.

A glass/Indium Tin Oxide (ITO) substrate is used as gate-functionalized support of the OLET. The final device is composed by 8 similar OLETs as reported in Figure 2.

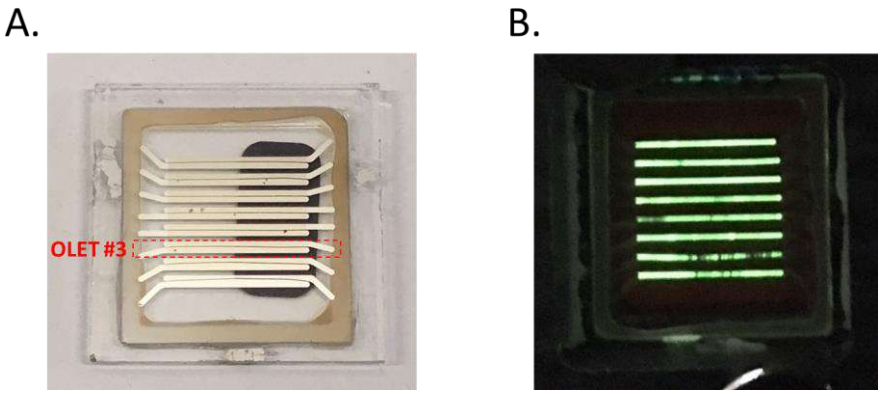

Figure 2. Picture of glass/ITO support (25mm x 25mm) containing 8 OLET devices in OFF state under ambient light illumination (a) and ON state in dark condition (b). As example, a red rectangle highlights the region of the OLET#3.

Green-emissive bilayer OLETs have been successfully fabricated at CNR and they represent benchmark devices for the development of OLETs to integrate in the MOLOKO sensor. The device architecture and the employed materials are shown in Figure 3. The parameters characterizing the electronic response of OLETs arise from the OFET technology and are: i) threshold gate voltage (V_{TH}), ii) hole mobility (μ_h), in the case of p-type OLETs, and iii) ON-OFF current ratio (I_{ON}/I_{OFF}). Concerning the optical characteristics of the devices, the main parameters to investigate are: *i)* the optical power, indicating the number of emitted photons, and the electroluminescence spectrum for the spectral response. In addition, the external quantum efficiency (EQE), defined as the ratio of the outcoupled photons to the injected charges, defines the efficiency of the device to convert current into light, depending on the externally applied bias.

In the case of benchmark green-emissive OLETs, as reported in D1.1, the device characteristics are the following:

- ☐ optical power ≈ 350 nW (in saturation regime at $V_{gate\text{-}source}$ = -100 V)
- ☐ $\mu_h \approx 2 \cdot 10^{-1}$ $cm^2 \cdot V^{-1} \cdot s^{-1}$
- ☐ V_{TH} (for holes) ≈ -35 V
- ☐ $I_{ON}/I_{OFF} \approx 10^6$

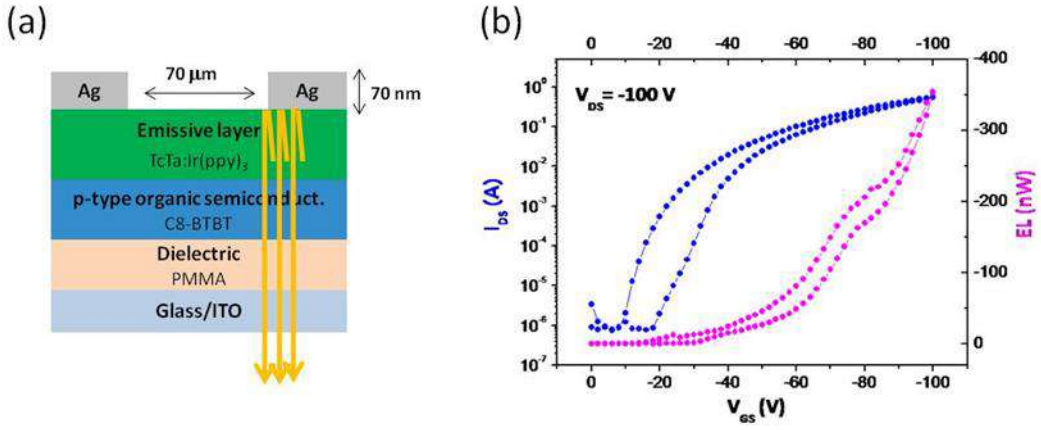

Figure 3. Representation of the device structure of a green-emissive OLET reporting the employed materials (a) and the corresponding I-V (blue dots) and optical power (pink dots) curves measured in saturation regime ($V_{drain\text{-}source}$ = -100 V) (b).

3 OLET development for MOLOKO application

In view of the integration of OLETs in the optoplasmonic chip, the corresponding three components, *i.e.* OLET, OPD and nanoplasmonic grating, need to be suitably modified to effectively cooperate and ensure a high detection sensitivity. In this regard, the benchmark OLET structure presented in Figure 3 has been tuned in terms of spectral response. Details on the spectral evolution are reported in the following paragraph 3.1 "*Spectral characteristics*". Moreover, the implementation of the three components of the optoplasmonic chip presents both optical and geometrical constrains, as reported in D1.1. Hence, paragraph 3.2 describes the OLET architectures that have been investigated accordingly. Finally, in view of the in-field implementation of the MOLOKO sensor, the power consumption of the components needs to be evaluated and reduced as much as possible. In this sight, paragraph 3.3 shows preliminary results on the strategy to reduce the operating voltage of OLETs.

3.1 Spectral characteristics

Following the requirements of the nanoplasmonic grating reported in D1.1, three different emission regions have been selected and evaluated for the OLETs: emission peak centered at *i*) ≈650 nm, *ii*) ≈740 nm or *iii*) ≈770 nm, respectively named option 1, 2 and 3. The corresponding emissive layers are the following:

1. **Alq_3:PtOEP** (tris-(8-hydroxyquinoline)aluminium : platinumoctaethylporphyrin), 8% PtOEP.
2. **$Pt(pfrpz)_2$** (2-pyrazinylpyrazolate Pt(II))
3. **Alq_3:Pt(tpbp)** (Pt(II)–tetraphenyltetrabenzoporphyrin), 6% Pt(tpbp)

As a matter of fact, the reported options involve the achievement of near-infrared (NIR) OLETs, diversely from the green-emissive benchmark structure (Figure 3). Hence, by following the literature manufacturing procedures,[1-3] the three emissive options have been inserted in the OLET architecture and optimized in terms of optoelectronic response. According to this, the device structure has been also slightly tuned to improve the optical output of the devices. In detail, two electron injection layers (EILs) have been inserted between the drain electrode and the emissive layer (Figure 4). This method has been demonstrated to enhance the optical power and the EQE of OLETs by favouring the injection of minority charges in the emissive materials.[4]

All the details on the device architecture and the employed materials are reported in Figure 4 and Table 1.

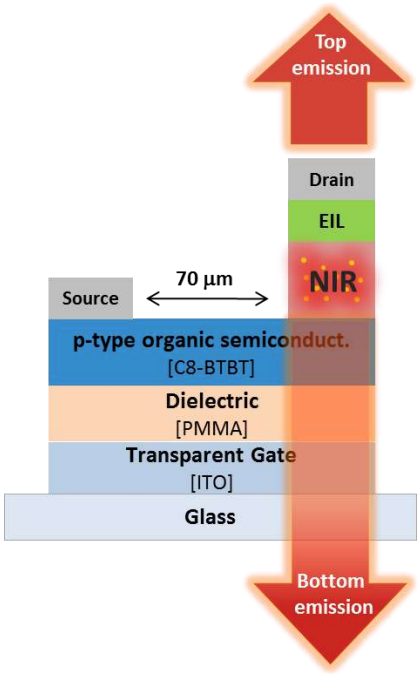

Figure 4. Schematic representation of the NIR-emitting OLET structure.

Table 1. Specification of the materials used in the NIR-emissive OLETs.

Layer type	*Material*	*Thickness*
Substrate	**Glass**	1.1 mm
Gate electrode	**ITO**	150 nm
Dielectric Material	Poly(methyl methacrylate) (**PMMA**)	450 nm
p-type organic semiconductor	2,7-Dioctyl[1]benzothieno[3,2-b][1]benzothiophene (**C8-BTBT**)	45 nm
NIR emitter option #1	**Alq_3:PtOEP**	30 nm
NIR emitter option #2	**$Pt(pfrpz)_2$**	20 nm
NIR emitter option #3	**Alq_3:Pt(tpbp)**	60 nm
EIL	Bilayer of: 1. 2,2',2"-(1,3,5-Benzinetriyl)-tris(1-phenyl-1-H-benzimidazole) (**TPBi**) 2. Cesium Carbonate (**Cs_2CO_3**)	1. = 40 nm 2. = few nm
Source electrode	**Silver**	70 nm
Drain electrode	**Silver**	14, 20, 70 nm

NIR option #1

The use, as emissive layer, of a blend of Alq_3:PtOEP (Table 1) resulted in OLETs emitting light at 645 nm with a narrow spectrum characterized by full width at half maximum (FWHM) of 20 nm (Figure 5a). The presence of a narrow emission represents an interesting characteristic of the corresponding OLETs since it would

ensure an extended spectral modulation by the nanoplasmonic grating in terms of emission peak position and FWHM, and thus high detection sensitivity.
In agreement with the literature,[4] the as-fabricated OLETs showed good characteristics as transistors (Figure 5b), with $\mu_h \approx 2x10^{-1}$ $cm^2V^{-1}s^{-1}$, $V_{th} \approx$ - 40V and $I_{ON}/I_{OFF} \approx 10^5$. In addition, optical power as high as 3 µW was measured at V_{DS} = -100V, V_{GS} = -100V. The optical power is a measure of the power of the light emission, thus indicating the number of photons emitted by the device. The value of optical power of 3 µW results higher than the optical power of internal references at CNR[4] and confirms the very good performance of the corresponding devices as light source.
Finally, by sweeping V_{DS} from -60V to -100V (in saturation transfer characteristics), OLETs reported EQEs in the range 0.2% - 0.5%. This parameter, which represents the efficiency of the device to convert charges into outcoupled photons, despite not at the forefront of the literature, demonstrates a fairly good performance of the reported OLETs. This means that, if required, further improvement of the OLET characteristics can be evaluated in view of the MOLOKO implementation. It is worth mentioning that there is poor correlation between the sensitivity of the optoplasmonic chip and the EQE of OLETs. Indeed, the sensitivity israther correlated to the amount of outcoupled photons, which is described by the great optical power of the device.

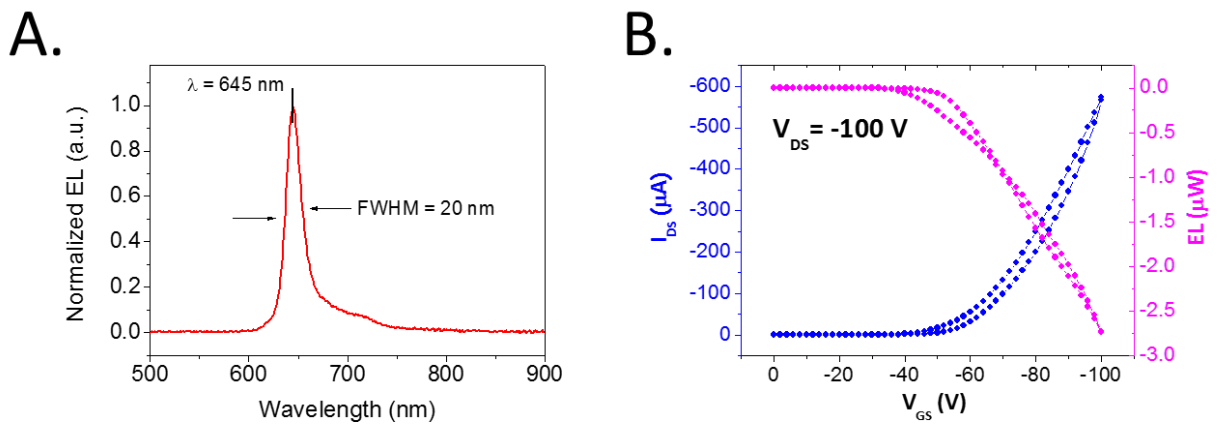

Figure 5. Electroluminescence spectrum of Alq_3:PtOEP- based OLETs (a) and the corresponding optoelectronics characterization (b): transfer I_{DS}-V_{GS} curve in saturation mode (blue dots) and optical power (pink dots).

NIR option #2

By using $Pt(pfrpz)_2$ as a single layer for NIR emission in OLETs (Figure 4), the corresponding devices showed good electrical characteristics as evidenced by $\mu_h \approx 2x10^{-1}$ $cm^2V^{-1}s^{-1}$, $V_{th} \approx$ - 40 V and $I_{ON}/I_{OFF} \approx 10^2$ (Figure 6b). If compared to Alq_3:PtOEP-based OLETs (Figure 5), the relatively low I_{ON}/I_{OFF} ratio of $Pt(pfrpz)_2$-based OLETs is maybe the evidence that the structure design still needs to be optimized. According to this, a relatively low optical power of ≈ 17 nW and an electroluminescence spectrum with FWHM over 140 nm (Figure 6) were measured. Nevertheless, the emission peak resulted at around 730 nm, quite similar to the value reported in the literature, *i.e.* 740 nm.[2] This highlights that, despite the fabrication protocol of $Pt(pfrpz)_2$-OLETs still need to be optimized to achieved higher optical response, the devices electrical performance and ability to emit light in the required spectral region is the proof that NIR emission at around 740 nm can be obtained and that option #2 (Table 1) is an available alternative in view of the optoplasmonic chip production.

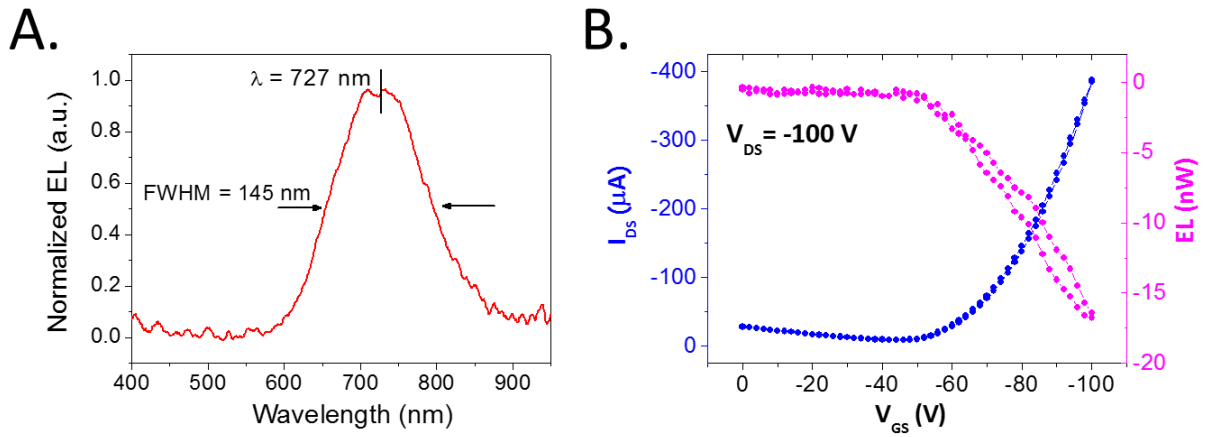

Figure 6. Electroluminescence spectrum of $Pt(pfrpz)_2$- based OLETs (a) and the corresponding optoelectronics characterization (b): transfer I_{DS}-V_{GS} curve in saturation mode (blue dots) and optical power (pink dots).

NIR option #3

OLETs including Alq_3:Pt(tpbp) as a host:guest emissive layer showed an electroluminescence peak at 766 nm (Figure 7a), in agreement with the corresponding OLED characteristics from the literature.[5] This confirms the good operation of OLET devices, where side mechanisms affecting their spectral response can be neglected. The FWHM resulted ≈ 40nm, suitable to ensure a good sensitivity of the optoplasmonic chip. 766-nm emitting OLETs reported a good behaviour as transistors, with $\mu_h \approx 2x10^{-1}$ $cm^2V^{-1}s^{-1}$, $V_{th} \approx$ - 40 V and $I_{ON}/I_{OFF} \approx 10^6$, similar to the characteristics of Alq_3:PtOEP-based OLETs (Figure 5b). Notably, the optical power resulted higher than 4 μW and the EQE, at V_{GS} from -60V to -100V, resulted in the range 1% - 0.5%. These values evidence the excellent operation of Alq_3:Pt(tpbp)-based OLETs and, by considering the good spectral overlap with the other optoplasmonic components (see D1.2), can be considered the best alternatives among the three selected options.

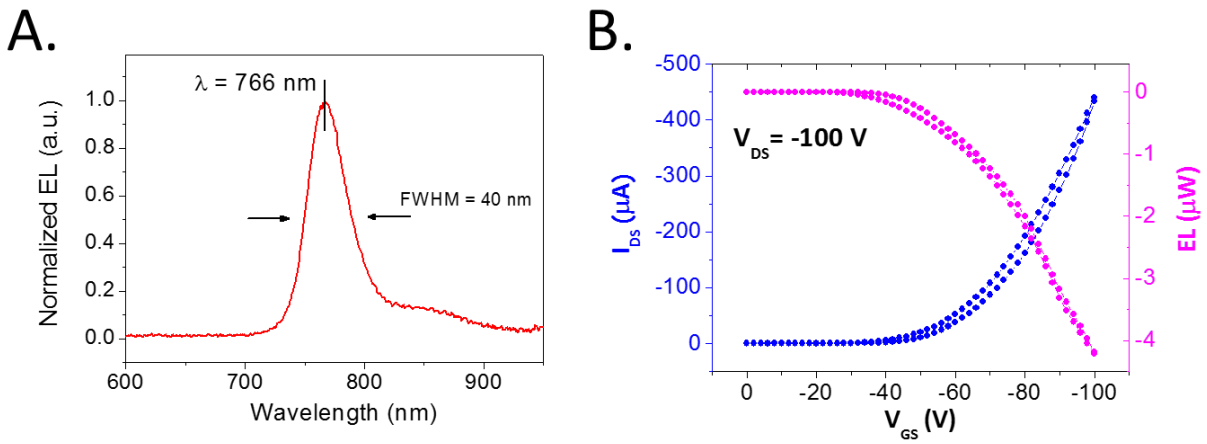

Figure 7. Electroluminescence spectrum of Alq_3: Pt(tpbp)- based OLETs (a) and the corresponding optoelectronics characterization (b): transfer I_{DS}-V_{GS} curve in saturation mode (blue dots) and optical power (pink dots)

3.2 Architectures

Concerning the optoplasmonic chip assembling, as defined in the specifications of D1.1, two main strategies are considered: **M1** "*Semitransparent Drain*" and **M2** "*Reflective encapsulation*".
According to strategy M1, the light generated by the OLET should reach the above-positioned nanoplasmonic grating, then modulated and back directed to the OPD, which is placed onto the OLET source electrode. A semi-transparent drain is therefore required for the OLET. In this regard, top-emitting devices have been developed. As preliminary approach, the protocol followed at CNR consisted in keeping constant the device structure while using a drain electrode as thin as possible.
Option #3 (766-nm emitting structure) was selected as benchmark OLET and different silver thicknesses of the drain electrode have been investigated. The use of a 14 nm-thick Ag electrode resulted in OLETs with similar characteristics to those already reported in Figure 7, with $\mu_h \approx 10^{-1}$ $cm^2V^{-1}s^{-1}$, $V_{th} \approx$ - 40 V and $I_{ON}/I_{OFF} \approx 10^5$. Despite the use of a thin silver layer as drain electrode, the OLET optical power resulted relatively low, with values of 150 nW from the OLET top side and 800 nW from the bottom side. In sight of this, the Ag thickness has been tuned and the optimized-drain layer, in terms of optoelectronic FOMs of the OLETs, resulted 20 nm-thick. Indeed, as shown in Figure 8b, electrical characteristics and optical power (measured from the bottom side of the OLETs) were similar to those of reference devices. In addition, the OLET optical power measured from the top side (Figure 8a) resulted only one order of magnitude lower than the corresponding optical power measured from the bottom side (at V_{DS} = -100V, V_{GS} = -100 V, optical power ≈ 500 nW and ≈ 5 µW when measured from the top and bottom OLET side, respectively) and three-times-higher than the optical power (measured from the top side) using 14 nm of Ag-drain.

Despite top-emitting OLETs can be further improved in terms of optical power, these preliminary tests highlight that both M1 and M2 strategies can be pursued if needed in view of the optoplasmonic chip assembling.

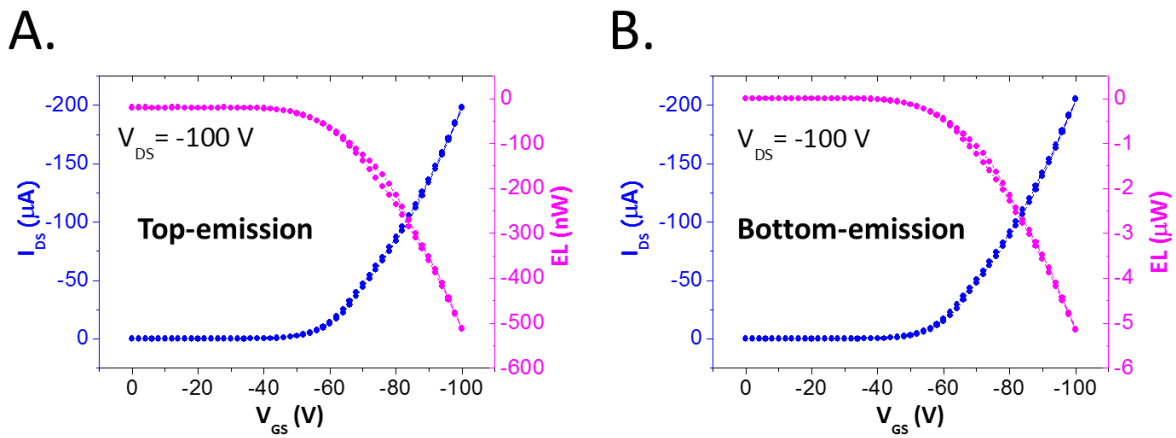

Figure 8. Saturation transfer I_{DS}-V_{GS} curves (blue dots), at VDS = -100 V, of 766nm-emitting OLETs and the corresponding optical power (pink dots) measured from the top (A) or the bottom (B) OLET side.

3.3 Operating conditions

In view of the OLET integration in the MOLOKO sensor, the power consumption of the whole device needs to be considered and kept as low as possible. In this regard, the OLET operating voltage plays an important role. In the here-reported results, OLETs start working at -40 V and show their best performance at -100 V in saturation mode (V_{DS} = -100 V).

At this stage of the project action, it is not mandatory to have low powered OLETs since the aim is the achievement of a monolithically integrated optoplasmonic chip where the OLET, the OPD and the nanoplasmonic grating cooperatively work to generate and detected light spectral modulation due to biological events. Nevertheless, preliminary tests to reduce the OLET operating voltage have been carried out. In particular, an Al_2O_3/PMMA bilayer was used as dielectric stack in the OLET structure reported in Figure 1, as replacement of a single layer of PMMA (Table 1). Indeed, Al_2O_3 is known to reduce the threshold voltage in OFETs and OLETs[6] if compared to devices using PMMA. The deposition of PMMA over Al_2O_3 is carried out to reduce the surface roughness and the number of traps, which typically affect the device response. By inserting the Al_2O_3/PMMA bilayer, OLETs operating at V_{GS} = -2V and with great optoelectronic performance at V_{GS} = -10 V have been obtained (Figure 9).

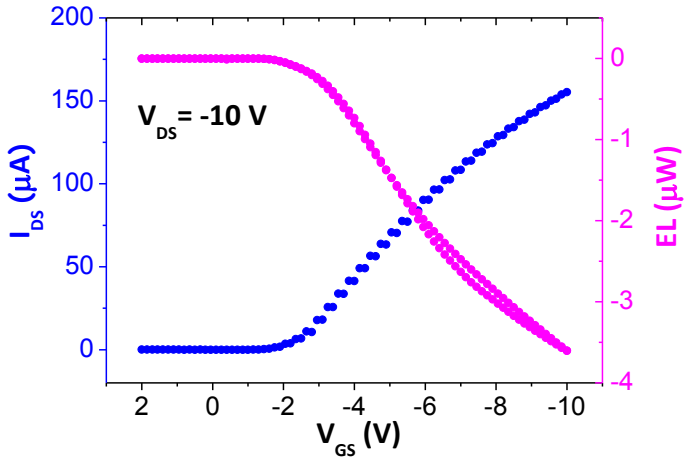

Figure 9. Transfer I_{DS}-V_{GS} curve in saturation mode (blue dots) and optical power (pink dots) of green emissive TCTA:Ir(ppy)$_3$-based OLETs using the device structure shown in Figure 1.

4 Conclusions

In the framework of Task 2.1 "*OLET Development*" of WP2, CNR focused on the fabrication, characterization, optimization and development of the OLET technology in view of the MOLOKO sensor integration. In particular, in jointly collaboration with PLASMORE and Fraunhofer-FEP, CNR successfully achieved three different OLET architectures emitting light at ≈650 nm, ≈740 nm and ≈770 nm. Indeed, in agreement with the requirement of the OPD and the nanoplasmonic grating, new emissive materials have been implemented in the OLET devices in order to allow the efficient and effective functioning of the whole optoplasmonic chip. The goal has been achieved through the fabrication and characterization of the figures-of-merit of each single device and the hence by improving the device characteristics in agreement with requirements the previously defined in D1.1.

According to the strategies M1 and M2 described and discussed in D1.1 for the optoplasmonic components assembly, operating devices with both top and bottom emission have been obtained.

In addition to that, in view of the final application of the whole MOLOKO sensor, preliminary results have been achieved on the reduction of the operating voltage of OLETs. In particular, devices working at a bias < |-10| V were demonstrated.

5 References

[1] C. Soldano, G. Generali, E. Cianci, G. Tallarida, M. Fanciulli and M. Muccini, Organic Light Emitting Transistors (OLETs) using ALD-grown Al_2O_3 dielectric, Society for Information Display International Symposium Digest of Technical Papers, 2016, https://doi.org/10.1002/sdtp.11049.

[2] K.T. Ly, R. Chen-Cheng, H. Lin, Y. Shiau, S. Liu, P. Chou, C. Tsao, Y. Huang and Y. Chi, Near-infrared organic light-emitting diodes with very high external quantum efficiency and radiance, Nature Photonics, 2017, 11, 63.

[3] C. Borek, K. Hanson, P.I. Djurovich, M.E. Thompson, K. Aznavour, R.Bau, Y. Sun, S.R. Forrest, J. Brooks, L. Michalski and J. Brown, Highly Efficient, Near-Infrared Electrophosphorescence from a Pt–Metalloporphyrin Complex. Angewandte Chemie, 2007, 119, 1127.

[4] M. Prosa, E. Benvenuti, M. Pasini, U. Giovanella, M. Bolognesi, L. Meazza, F. Galeotti, M. Muccini and S. Toffanin, ACS Appl. Mater. Interfaces, 2018, 10, 25580.

[5] Y. Sun, C. Borek, K. Hanson, P. I. Djurovich, M. E. Thompson, J. Brooks, J. J. Brown and S. R. Forrest, Appl. Phys. Lett. 2007, 90, 213503.

[6] M. Ullah, R. Wawrzinek, F. Maasoumi, S. Lo and E. B. Namdas, Adv. Optical Mater. 2016, 4, 1022.